ABUNDANCE GRADIENTS AND THE ROLE OF SNE IN M87/VIRGO

F. Gastaldello[1,2] and S. Molendi[1]

[1]IASF-CNR, via Bassini 15, I-20133 Milano, Italy
[2]Università di Milano Bicocca, Dip. di Fisica, P.za della Scienza 3 I-20133 Milano, Italy

arXiv:astro-ph/0202020v1 1 Feb 2002

Abstract

We make a detailed measurement of the metal abundance profiles and metal abundance ratios of the inner core of M87/Virgo observed by *XMM-Newton* during the PV phase. We use multi temperature models for the inner regions and we compare the plasma codes APEC and MEKAL. We confirm the strong heavy elements gradient previously found by *ASCA* and *BeppoSAX*, but also find a significant increase in light elements, in particular O. This fact together with the constant O/Fe ratio in the inner 9 arcmin indicates an enhancement of contribution in the core of the cluster not only by SNIa but also by SNII.

Key words: X-rays: galaxies — Galaxies: clusters — Galaxies: individual: M87 — Galaxies: abundances

1. Introduction

The study of metallicity in clusters of galaxies dates back to 1976, with the detection of the 7 keV blend line emission due to highly ionized iron as a strong feature in the X-ray spectra of the Perseus cluster (Mitchell et al. 1976). This was a most significant observational discovery concerning X-ray clusters, following their identification as X-ray sources, because it established without doubt that the primary emission mechanism was thermal and that the hot intra-cluster gas contained a significant portion of processed gas, which had at some point been ejected from stars (Sarazin 1988).

The X-ray emitting hot intra-cluster medium (ICM) of clusters of galaxies is now known to contain a large amount of metals: for rich clusters between red-shift 0.3-0.4 and the present day the observed metallicity is about 1/3 the solar value (Mushotzky & Lowenstein 1997, Allen & Fabian 1998, Fukazawa et al. 1998, Della Ceca et al 2000, Ettori et al. 2001), suggesting that a significant fraction of the ICM has been processed into stars already at intermediate red-shifts.
The total mass of iron is directly proportional to the optical luminosity from elliptical and lenticular galaxies, this fact strongly arguing for the metals now in the ICM having been produced by the massive stars of the same stellar population to which belong the low mass stars now producing the bulk of the cluster optical light (Arnaud et al. 1992, Renzini et al. 1993).

While the origin of the metals observed in the ICM is clear (they are produced by supernovae, in particular SNII and SNIa), less clear is the transfer mechanism of these metals to the ICM. The main mechanisms that have been proposed for the metal enrichment in clusters are: enrichment of gas during the formation of the proto-cluster (Kauffman & Charlot 1998); ram pressure stripping of metal enriched gas from cluster galaxies (Gunn & Gott 1972, Toniazzo & Schindler 2001); stellar winds AGN- or SN-induced in Early-type galaxies (Matteucci & Vettolani 1988, Renzini 1997).

Another controversial subject is the relative contribution to the metal enrichment by the two types of supernovae, SNIa and SNII. Mushotzky et al. (1996) and Mushotzky & Lowenstein (1997) showed a dominance of SNII ejecta, while other works on *ASCA* data (Ishimaru & Arimoto 1997, Fukazawa et al. 1998, Finoguenov et al 2000, Dupke & White 2000a), still indicating a predominance of SNII enrichment at large radii in clusters, do not exclude that as much as 50% of the iron in clusters come from SNIa ejecta in the inner part of clusters.

Spatially resolved abundance measurement in galaxy clusters are of great importance because they can be used to measure the precise amounts of metals in the ICM and to constrain the origin of metals both spatially and in terms of the different contributions of the two different type of SNe (since SNIa products are iron enriched, while SNII products are rich in α elements such as O, Ne, Mg and Si) as a function of the position in the cluster. The first two satellites able to perform spatially resolved spectroscopy, *ASCA* and *BeppoSAX* have revealed abundance gradients in cD clusters (Dupke & White 2000b, De Grandi & Molendi 2001), in particular M87/Virgo (Matsumoto et al. 1996, Guainazzi & Molendi 2000), and variations in Si/Fe within a cluster (Finoguenov et al 2000) and among clusters (Fukazawa et al. 1998). Given the diversity of metals produced by SNIa and SNII, the variations in Si/Fe suggest that the metals in the ICM have been produced by a mix of the two types of SNe.
Moreover with the aid of observational data on many elements, X-ray observation can discriminate between competing theoretical models for SNIa also because the central region of cD clusters, where the SNIa products could dom-

Proc. Symposium *'New Visions of the X-ray Universe in the XMM-Newton and Chandra Era'* 26–30 November 2001,

inate in the abundance pattern, can be considered as the archives of an extremely large number of SNIa explosions (Dupke & White 2000b, Finoguenov et al 2001).

The broad bandpass large X-ray sensitivity and good angular resolution of *XMM-Newton* enables the measurement of abundances and abundance gradients of elements that have not been accurately studied before. In particular the O abundance (and O/Fe ratio) is particularly important for estimation of the SNII contribution since O is expected to be produced mostly by this kind of supernova. Limited sensitivities of pre-*XMM-Newton* instruments for O VIII lines prevent this best measure to separate the enrichment by the two types of supernovae.

M87 is the cD galaxy of the nearest cluster and its high flux and close location makes it one of the most ideal target for a detailed study of the ICM abundance down to the scale of the kpc. Throughout this paper, we assume $H_0 = 50\,\mathrm{km\,s^{-1}Mpc^{-1}}$, $q_0 = 0.5$ and at the distance of M87 $1'$ corresponds to 5 kpc.

2. Observation and Data Preparation

M87/Virgo was observed with *XMM-Newton* (Jansen et al. 2001) during the PV phase with the MOS detector in Full Frame Mode for an effective exposure time of about 39 ks. Details on the observation have been published in Böhringer et al. (2001) and Belsole et al. (2001). We have obtained calibrated event files for the MOS1 and MOS2 cameras with SASv5.0. Data were manually screened to remove any remaining bright pixels or hot column. Periods in which the background is increased by soft proton flares have been excluded using an intensity filter: we rejected all events accumulated when the count rates exceeds 15 cts/100s in the $[10-12]$ keV band for the two MOS cameras.

We have accumulated spectra in 10 concentric annular regions centered on the emission peak extending our analysis out to 14 arcmin from the emission peak, thus exploiting the entire *XMM* field of view. We have removed point sources and the substructures which are clearly visible from the X-ray image (Belsole et al. 2001) except in the innermost region, where we have kept the nucleus and knot A, because on angular scales so small it is not possible to exclude completely their emission. We prefer to fit the spectrum of this region with a model which includes a power law component to fit the two point like sources. We include only one power law component due to the similarity of the two sources spectra (Böhringer et al. 2001). The bounding radii are $0'$-$0.5'$, $0.5'$-$1'$, $1'$-$2'$, $2'$-$3'$, $3'$-$4'$, $4'$-$5'$, $5'$-$7'$, $7'$-$9'$, $9'$-$11'$ and $11'$-$14'$. The analysis of the 4 central regions within 3 arcmin was already discussed in Molendi & Gastaldello (2001).

Spectra have been accumulated for MOS1 and MOS2 independently. The Lockman Hole observations have been used for the background. Background spectra have been accumulated from the same detector regions as the source spectra.

The vignetting correction has been applied to the spectra rather than to the effective area, as is customary in the analysis of EPIC data (Arnaud et al. 2001). Spectral fits were performed in the 0.5-4.0 keV band. Data below 0.5 keV were excluded to avoid residual calibration problems in the MOS response matrices at soft energies. Data above 4 keV were excluded because of substantial contamination of the spectra by hotter gas emitting further out in the cluster, on the same line of sight.

As discussed in Molendi (2001) there are cross-calibration uncertainties between the spectral response of the two EPIC instruments, MOS and PN. In particular for what concern the soft energy band (0.5-1.0 keV) fitting six extra-galactic spectra for which no excess absorption is expected, MOS recovered the N_H galactic value, while PN gives smaller N_H by $1-2\times10^{20}\mathrm{cm^{-2}}$. Thus we think that at the moment the MOS results are more reliable than the PN ones in this energy band, which is crucial for the O abundance measure. For this reason and for the better spectral resolutions of MOS, which is again important in deriving the O abundance, we limit our analysis to MOS data.

3. Spectral modeling and plasma codes

The X-ray emission in cluster of galaxies originates from the hot gas permeating the cluster potential well. The continuum emission is dominated by thermal bremsstrahlung, which is proportional to the square of the gas density times the cooling function. From the shape and the normalization of the spectrum we derive the gas temperature and density. In addition the X-ray spectra of clusters of galaxies are rich in emission lines due to K-shell transitions from O, Ne, Mg, Si, S, Ar and Ca and K- and L-shell transitions from Fe and Ni, from which we can measure the relative abundance of a given element. A measure of the equivalent width of a spectral line is a direct measure of the relative abundance of a given element. This comes from the fact that both the continuum and line emission are two body processes with the continuum emissivity proportional to the electron density times the proton density and the line emissivity proportional to the electron density times the density of a given element. From the definition of equivalent width it is easily derived that this quantity is proportional to the ratio between the ion and proton densities.

In Figure 1 we show the data of the $3'$-$4'$ bin together with the best fitting model calculated using the MEKAL code. The model has been plotted nine times, each time all element abundances, except one, are set to zero. In this way the contribution of the various elements to the observed lines and line blends become apparent. In the energy band (0.5-4 keV) we have adopted for the spectral fitting, the abundance measurements based on K-lines for all the elements except for Fe and Ni, for which the measure is based on L-lines. The K-lines of O, Si, S, Ar and Ca are well isolated from other emission features and clearly separated from the continuum emission, which are the requirements for a robust measure of the equivalent width of the lines and consequently of the abundances of these elements. The Fe-L lines are known to be problematic, because the atomic physics involved is more complicated than K-shell transitions (Liedahl et al. 1995, but from the very good signal of *XMM* spectra and from the experience of *ASCA* data (Mushotzky et al. 1996, Hwang et al. 1997, Fukazawa et al. 1998) we can conclude that the Fe-L determination is reliable. Some of the stronger Fe-L lines due to Fe XXII and Fe XXIV are close to the K-lines of Ne and Mg, respectively and blending can lead to errors in the Ne abundance and, to a smaller extent, to the Mg abundance (Liedahl et al. 1995, Mushotzky et al. 1996). Also the Ni measure is difficult due to the possible confusion of its L-lines with the continuum and Fe-L blend.

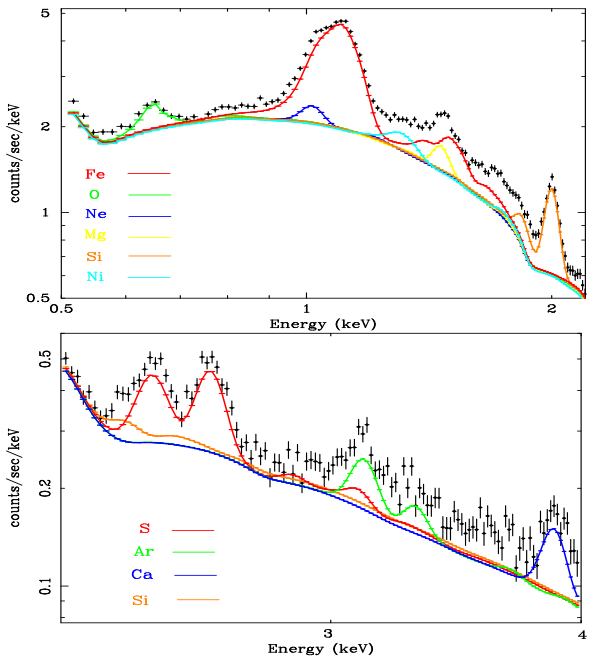

Figure 1. Data of the 3′-4′ bin and lines of the various elements, obtained by setting all element abundances to zero except the one of interest, calculated using the MEKAL code.
Top Panel*: the lines of O, Fe, Ne, Ni, Mg and Si used for the analysis in the 0.5-2 keV energy range.*
Bottom Panel*: the lines of Si, S, Ar and Ca used for the analysis in the 2-4 keV energy range.*

The elemental abundances are expressed by the relative values to the solar abundances from Grevesse & Sauval (1998) that updates the commonly used values from Anders & Grevesse (1989)

All spectral fitting has been performed using version 11.0.1 of the XSPEC package.

All models discussed below include a multiplicative component to account for the galactic absorption on the line of sight of M87. The column density is always fixed at a value of 1.8×10^{20} cm^{-2}, which is derived from 21cm measurements (Lieu et al. 1996). Leaving N_H to freely vary does not improve the fit and does not affect the measure of the oxygen abundance, which could have been the more sensitive to the presence of excess absorption. The N_H value obtained is consistent within the errors with the 21cm value.

The temperature profile for M87 (Böhringer et al. 2001 shows a small gradient for radii larger than $\sim$ 2 arcmin and a rapid decrease for smaller radii. Moreover, as pointed out in Molendi & Pizzolato (2001) all spectra at radii larger than 2 arcmin are characterized by being substantially isothermal (although the spectra of the regions between 2 and 7 arcmin are multi temperature spectra with a narrow temperature range rather than single temperature spectra), while at radii smaller than 2 arcmin we need models which can reproduce the broad temperature distribution of the inner regions.

We therefore apply to the central regions (inside 3 arcmin) three different spectral models.

A two temperature model (vmekal + vmekal in XSPEC and model II in (Molendi & Gastaldello 2001) using the plasma code MEKAL (Mewe et al. 1985, Liedahl et al. 1995). The metal abundance of each element of the second thermal component is bound to be equal to the same parameter of the first thermal component. This model is used (e.g. Makishima et al. (2001) and refs. therein) as an alternative to cooling-flow models in fitting the central regions of galaxy clusters.

A "fake multi-phase" model (vmekal + vmcflow in XSPEC and model III in Molendi & Gastaldello (2001). As indicated in recent papers (Molendi & Pizzolato 2001, Molendi & Gastaldello 2001) this model is used to describe a scenario different from a multi-phase gas, for which it was written for: the gas is all at one temperature and the multi-phase appearance of the spectrum comes from projection of emission from many different physical radii. A more correct description will be given by a real deprojection of the spectrum.

The third model is the analogue of the vmekal two temperature model using the plasma code APEC (Smith et al. 2001).

We can't adopt an APEC analogue of the fake multi-phase model because the cooling flow model calculating its emission using APEC is still under development. Given the substantial agreement between 2T and fake multi-phase model (Molendi & Gastaldello 2001), we can regard the 2T APEC results as indicative also for a fake multi-phase model.

For the spectrum accumulated in the innermost region we included also a power law component to model the emission of the nucleus and of knot A.

For what concern the measure of metal abundances, it is crucial to use multi temperature models in the inner bins, where the evidence of multi temperature gas is stronger. Infact single temperature models substantially underestimate the metal abundance in multi temperature spectra, as already observed in ASCA spectra of galaxies and galaxy groups (Fe bias: Buote 2000). In M87 the drastic abundance decrement found in the previous analysis (Böhringer et al. 2001) follows from the application of the oversimplified single temperature model (Molendi & Gastaldello 2001), as shown in Figure 2.

For the outer regions (from 3 arcmin outwards) we apply single temperature models: vmekal using the MEKAL code and vapec using the APEC code.

We use the two different plasma codes with the aim of cross-checking their results. As pointed out by the authors of the new code APEC, cross-checking is very important, since each plasma emission code requires choosing from a large overlapping but incomplete set of atomic data and the results obtained by using independent models allows critical comparison and evaluation of errors in the code and in the atomic database.

4. Results

4.1. Abundance profiles

The abundance measurements obtained using the two different plasma codes agree for what concerns Fe, Ar and Ca; they are somewhat different for what concerns O, S and Ni and in complete disagreement for Mg and Ne. The temperature profile obtained with the two codes are somewhat different in the inner regions (where we compare the range of temperature ob-

tained by multi-temperature models), while there is substantially agreement in the outer isothermal bins.

The models using the APEC code give a systematically worse description than the ones using MEKAL code; we show some examples in Fig. 3. In the external bins the differences in the fit between the two codes are due to APEC over-prediction of the flux of Fe-L lines from high ionization states, considering the fact that the temperature obtained by the two codes are nearly coincident. For the inner regions the differences between the two codes are further complicated by the different temperature range they find for the best fit. In general, where the temperature structure is very similar, as in the innermost bin, the difference is as in the outer bins in the high energy part of the Fe-L blend, while where the temperature structure is different, as in the $1'$-$2'$ shown in Figure 3, the differences between the two codes are primary due to different estimates of the flux of He-like Si-K line.

We therefore choose as our best abundance profiles those obtained with a 2T vmekal fit for the central regions and with a 1T vmekal fit for the outer regions. We report the abundance profiles obtained in this way in Fig 4 for O, Si, Fe, in Fig 5 for Mg, Ar, S and in Fig 6 for Ne, Ca, Ni. Abundance gradients are clearly evident for Fe, Si, S, Ar and Ca; a statistically significant enhancement is evident in the central regions for O, Mg and Ni, while only Ne is substantially flat.

4.2. Abundance ratios

From the abundance measurements we obtain the abundance ratios between all the elements relative to Fe, normalized to the solar value. As an example we show the two more significant abundance ratios, O/Fe and S/Fe, in Fig. 7, together with the abundance ratios obtained by models of supernovae taken by Nomoto et al. (1997) and rescaled to the solar abundances reported in Grevesse & Sauval (1998).

An important results is the constance in the inner 9 arcmin of the ratio O/Fe (fitting the data with a constant gives $\chi^2 = 6.9$ for 7 d.of. and adding a linear component does not improve the fit, $\chi^2 = 5.4$ for 6 d.o.f) which, together with the enhancement in the O abundance in the inner regions points towards an increase in contribution by SNII, since O is basically produced only by this kind of supernovae.

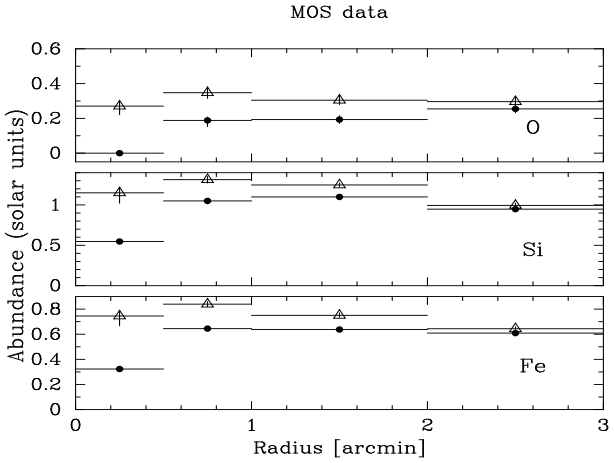

Figure 2. Abundance profiles for O, Si and Fe in the inner 3 arcmin. Full circles indicate the measurements with a single temperature model, while empty triangles those with a two temperature model. Solar units are the old ones by Anders & Grevess (1989).

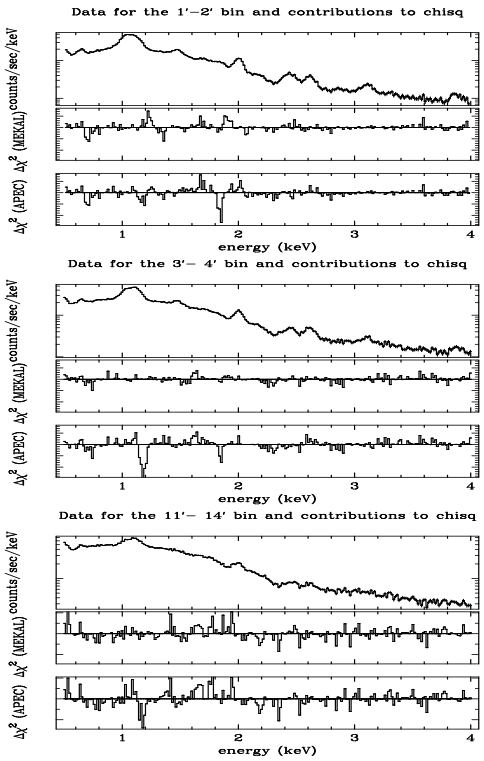

Figure 3. **Top Panel***: data for the bin $1'$-$2'$ and contributions to χ^2 for a 2T model with MEKAL code, the χ^2/d.o.f. of the fit is 381/217, and for a 2T model with APEC code, the χ^2/d.o.f. of the fit is 474/218. Contributions to χ^2 are on the same scale for direct comparison.*
Middle Panel*: data for the bin $3'$-$4'$ and contributions to χ^2 for a 1T model with MEKAL code, the χ^2/d.o.f. of the fit is 326/221, and for a 1T model with APEC code, the χ^2/d.o.f. of the fit is 546/222. Contributions to χ^2 are on the same scale for direct comparison.*
Bottom Panel*: data for the bin $11'$-$14'$ and contributions to χ^2 for a 1T model with MEKAL code, the χ^2/d.o.f. of the fit is 729/221, and for a 1T model with APEC code, the χ^2/d.o.f. of the fit is 886/222. Contributions to χ^2 are on the same scale for direct comparison.*

The ratio S/Fe, and in general M87 data, suggests an agreement with delayed detonation models (in particular for the inner bins), as stressed by Finoguenov et al (2001). If we consider the set of theoretical values for SNII and W7 SNIa models the behavior of these ratio would indicate an increasing contribution by SNIa going *outward* to the center. We recover the correct behavior if we choose the WDD1 yield and we reduce the S SNII yield of Nomoto et al. (1997) by a factor of two to three, as was already indicated by ASCA data (Dupke & White 2000a).

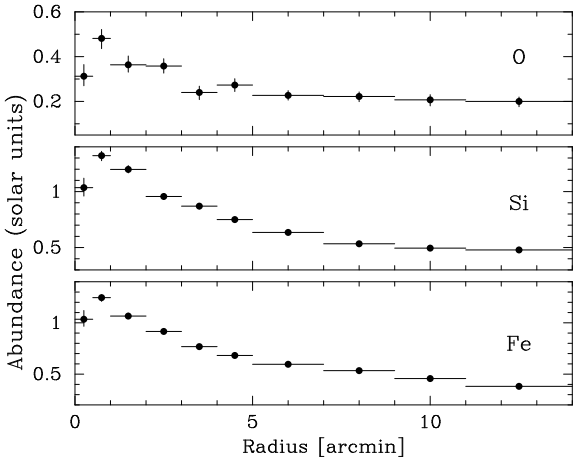

Figure 4. MOS abundance profiles for O, Si and Fe, obtained with a 2T model using MEKAL code for the inner 3 arcmin and with a 1T model using MEKAL code for the outer bins. Uncertainties are at the 68% level for one interesting parameter($\Delta\chi^2 = 1$).

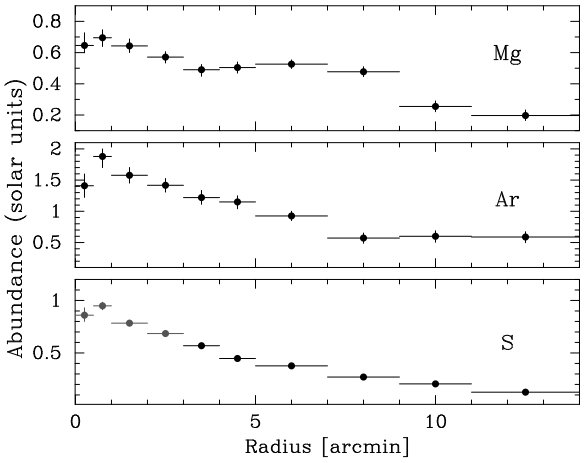

Figure 5. Same as Fig. 4 but for Mg, Ar and S.

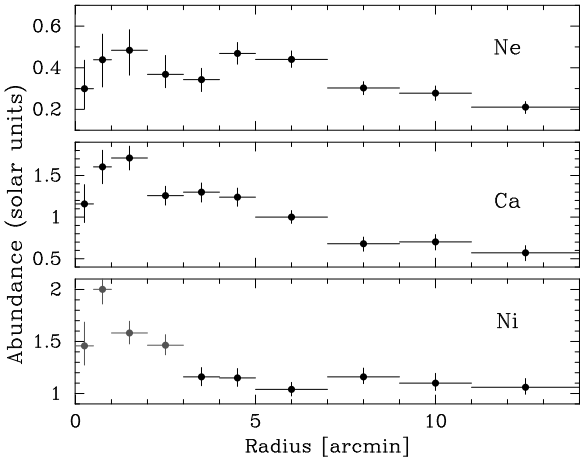

Figure 6. Same as Fig. 4 but for Ne, Ca and Ni.

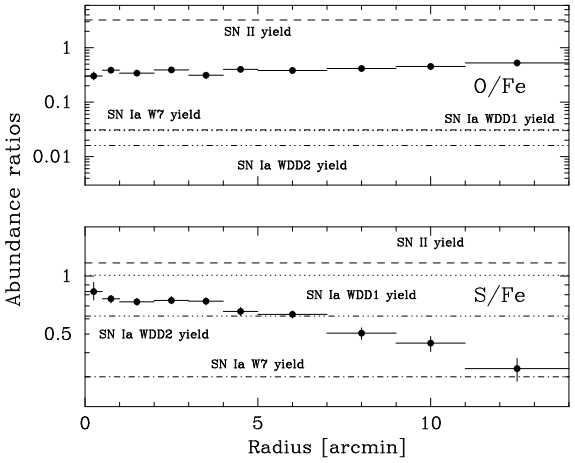

Figure 7. MOS abundance ratio profiles for O/Fe and S/Fe. Also showed are the abundance ratios predicted by SNe models taken by Nomoto et al. 1997: the dashed line refers to the SNII model, the dash-dotted line to the W7 SNIa model, the dotted line to the WDD1 SNIa model and the three dotted-dashed line to the WDD2 SNIa model.

5. Discussion

The model emerging from the *ASCA* and *BeppoSAX* data for the explanation of abundance gradients in galaxy clusters was that of a homogeneous enrichment by SNII, the main source of α elements, maybe in the form of strong galactic winds in the proto-cluster phase and the central increase in the heavy element distribution due to an enhanced contribution by SNIa, strongly related to the presence of a cD galaxy (Fukazawa et al. 1998, Dupke & White 2000b, Finoguenov et al 2000, De Grandi & Molendi 2001, Makishima et al. 2001). As a textbook example we can consider the case of A496 observed by *XMM-Newton* (Tamura et al. 2001). The O-Ne-Mg abundance is radially constant over the cluster, while the excess of heavy elements as Fe, Ar, Ca and Ni in the core is consistent with the assumption that the metal excess is solely produced by SNIa in the cD galaxy. The crucial ratio for the discrimination of the enrichment by the two types of supernovae, O/Fe, is then decreasing towards the center.

The XMM results for M87/Virgo complicates this picture. Together with the improved accuracy in the measure of the heavy elements gradients, showing the increased contribution by SNIa, the statistically significant enhancement of α elements O and Mg and the constant O/Fe ratio point toward an increase in contribution also of SNII. A mechanism which enhances the contribution of SNII over the homogeneous contribution all over the cluster must have been at work in the center of the cluster. Although there is little or no evidence of current star formation in the core of M87, the O excess could be related to a recent past episode of star formation triggered by the passage of the radio jet, as we see in cD galaxies with a radio source (A1795 cD: van Breugel et al. 1984 and A2597 cD: Koekemoer et al. 1999), nearby (Cen A: Graham 1998) and distant radio galaxies (van Breugel et al. 1985, van Breugel & Dey 1993, Bicknell et al. 2000) (for a comprehensive discussion see McNamara 1999).

To put the above idea quantitatively, waiting for a true deprojection of our data, we use previous ROSAT estimate of the deprojected electron density in the center of the Virgo cluster (Nulsen & Böhringer 1995) to calculate the excess mass of oxygen. To estimate the excess abundance we fit the inner bins, where we see the stronger increase in the O abundance, with a constant obtaining an abundance of 0.32, while for the outer bins we obtain an abundance of 0.21 so the excess is 0.11. Then we estimate the oxygen mass, $M_{\rm O}$ to be $M_{\rm O} = A_{\rm O}\, y_{\rm O,\odot}\, Z_{\rm O}^{excess}\, M_H$, where $M_H = 0.82\, n_e\, \frac{4\pi}{3}\, (R_{out} - R_{in})^3$, R_{in} and R_{out} being the bounding radii in kpc of the bins, $A_{\rm O} = 16$ and $y_{\rm O,\odot} = 6.76 \times 10^{-5}$ from Grevesse & Sauval (1998). We obtain a rough estimate of $10^7\,{\rm M}_\odot$ which, assuming that about $80\,{\rm M}_\odot$ of star formation are required to generate a SNII (Thomas & Fabian 1990) and Nomoto SNII oxygen yield, requires a cumulative star formation of $4 - 5 \times 10^7\,{\rm M}_\odot$. This star formation is in agreement with a burst mode of star formation ($\sim 10^7$ yr) at rates of $\sim 10 - 40\,{\rm M}_\odot\,{\rm yr}^{-1}$, as it is observed in the CD galaxies of A1795 and A2597 (McNamara 1999).

Acknowledgements

This work is based on observations obtained with *XMM-Newton*, an ESA science mission with instruments and contributions directly funded by ESA Member States and the USA (NASA).

References

Allen, S. W. & Fabian, A. C. 1998, MNRAS, 297, L63
Anders, E. & Grevesse, N. 1989, Geochimica et Cosmochimica Acta, 53, 197
Arnaud, M., Rothenflug, R., Boulade, O., Vigroux, L., Vangioni-Flam, E., 1992, A&A, 254, 49
Arnaud, M., Neumann, D. M., Aghanim, N., Gastaud, R., Majerowicz, S., Hughes, J. P. 2001, A&A, 365, L80
Belsole, E., Sauvageot, J. L., Böhringer, H., Worral, D. M., Matsushita, K., Mushotzky, R. F., Sakelliou, I., Molendi, S., Ehle, M., Kennea, J., Stewart, G., Vestrand, W. T. 2001, A&A, 365, L188
Bicknell, G., Sutherland, R., van Breugel, W.J.M., Dopita, M.A., Dey, A, Miley, G.K. 2000, ApJ, 540, 678
Böhringer, H., Belsole, E., Kennea, J., Matsushita, K., Molendi, S., Worral, D. M., Mushotzky, R. F., Ehle, M., Guainazzi, M., Sakelliou, I., Stewart, G., Vestrand, W. T., Dos Santos, S. 2001, A&A, 365 L181
Buote, D.A., 2000, ApJ, 539, 172
De Grandi, S. & Molendi, S. 2001, ApJ, 551, 153
Della Ceca, R., Scaramella, R., Gioia, I. M., Rosati, P., Fiore, F., Squires, G. 2000, A&A, 353, 498
Dupke, R. A. & White R. 2000a, ApJ, 528, 139
Dupke, R. A. & White R. 2000b, ApJ, 537, 123
Ettori, S., Allen, S. W., Fabian, A. C. 2001, MNRAS, 322, 187
Finoguenov, A., David, L. P., Ponman, T. J. 2000, ApJ, 544, 188
Finoguenov, A., Matsushita, K., Böhringer, H., Ikebe, Y., Arnaud, M. 2001, A&A in press, (astro-ph/0110516)
Fukazawa, Y., Makishima, K., Tamura, T., Ezawa, H., Xu, H., Ikebe, Y., kikuchi, K., Ohashi, T. 1998, PASJ, 50, 187
Graham, J.A., 1998, ApJ, 502, 245
Gibson, B. K., Lowenstein, M., Mushotzky, R. F. 1997, MNRAS, 290, 623
Grevesse, N. & Sauval, A. J., 1998, Space Science Reviews, 85, 161
Guainazzi, M. & Molendi, S. 2000, A&A, 351, L19
Gunn, J. E. & Gott, J. R. 1972, ApJ, 176, 1
Hwang, U., Mushotzky R., Loewenstein, M., Markert, T. H., Fukazawa, Y., Matsumoto, H. 1997, ApJ, 476, 560
Kauffmann, G. & Charlot, S. 1998, MNRAS, 294, 705
Koekemoer, A.M., O'Dea, C.P., Sarazin, C.L., McNamara, B.R., Donahue, M., Voit, G.M., Baum, S.A., Gallimore, J.F., ApJ, 525, 621
Jansen, F., Lumb, D., Altieri, B., Clavel, J., Ehle, M., Erd, C., Gabriel, C., Guainazzi, M., Gondoin, P., Much, R., Munoz, R., Santos, M.,Schartel, N., Texier, D., Vacanti, G. 2001, A&A, 365, L1
Ishimaru, Y. & Arimoto, N. 1997, PASJ, 49,1
Liedahl, D. A., Osterheld A. L., Goldstein, W. H. 1995, ApJ, 438, L115
Lieu, R., Mittaz, J. P. D., Bowyer, S., Lockman, F. J., Hwang,, C. Y., Schmitt, J. H. M. M. 1996, ApJ, 458, L5
Makishima, K., Ezawa, H., Fukazawa, Y., Honda, H., Ikebe, Y., Kamae, T., Kikuchi, K., Matsushita, K., Nakazawa, K., Ohashi, T., Takahashi, T., Tamura, T., Xu, H. 2001, PASJ, 53, 401
Matsumoto, H., Koyama, K., Awaki, H., Tomida, H., Tsuru, T., Mushotzky, R., Hatsukade, I. 1996, PASJ, 48, 201
Matteucci, F. & Vettolani, G. 1988, A&A, 202, 21
McNamara 1999, presented at "Life cycles of Radio Galaxies", July 15-17, 1999, STScI, Baltimore (astro-ph/9911129)
Mewe, R., Gronenschild, E. H. B. M., van den Oord, G. H. J., 1985, A&AS, 62, 197
Mitchell, R.J., Culhane, R.J., Davison, P.J., Ives, J.C., 1976, MNRAS, 176, 29p
Molendi, S., 2001, *Report on MOS PN cross-calibration presented at Leicester EPIC calibration meeting held in June 2001*
Molendi, S. & Gastaldello, F. 2001, A&A, 375, L14
Molendi, S. & Pizzolato, F. 2001, ApJ, 560, 194
Mushotzky, R., Loewenstein, M., Arnaud, K. A., Tamura, T., Fukazawa, Y., Matsushita, K., Kikuchi, K., Hatsukade, I. 1996, ApJ, 466, 686
Mushotzky, R. & Lowenstein, M. 1997, ApJ, 481, L63
Nomoto, K., Iwamoto, K., Nakasato, N., Thielemann, F. K., Brachwitz, F., Tsujimoto, T., Kubo, Y., Kishimoto, N. 1997, Nucl.Phys. A, 621, 467
Nulsen, P.E.J. & Böhringer, H., 1995, MNRAS, 274, 1093
Renzini, A., Ciotti, L., D'Ercole, A., Pellegrini, S., 1993, ApJ, 419, 52
Renzini, A., 1997, ApJ, 488, 35
Sarazin, C.L., X-ray emission from clusters of galaxies. Cambridge Univ. Press, Cambridge
Smith, R. K., Brickhouse, N. S., Liedahl, D. A., Raymond, J. C. 2001, ApJ, 556, L91
Tamura, T., Bleeker, A.M., Kaastra, J.S., Ferrigno, C., Molendi, S. 2001, A&A, 379, 107
Thomas, P.A. & Fabian, A.C., 1990, MNRAS, 246, 156
Toniazzo, T. & Schindler, S. 2001, MNRAS, 325, 509
van Breugel, W.J.M., Heckman, T., Miley, G. 1984, ApJ, 276, 79
van Breugel, W.J.M., Filippenko, A.V., Heckman, T., Miley, G. 1985, ApJ, 293, 83
van Breugel, W.J.M. & Dey, A. 1993, ApJ, 414, 563